

Axion Emission from Proton Cooper Pairs in Neutron Stars

Koichi Hamaguchi^{a,b*}, Natsumi Nagata^{a†}, and Jiaming Zheng[‡]

^a*Department of Physics, University of Tokyo, Bunkyo-ku, Tokyo 113-0033, Japan*

^b*Kavli IPMU (WPI), University of Tokyo, Kashiwa, Chiba 277-8583, Japan*

Abstract

We investigate axion emission from singlet proton Cooper pairs in neutron stars, a process that dominates axion emission in young neutron stars in the KSVZ model. By re-deriving its emissivity, we confirm consistency with most existing literature, except for a recent study that exhibits a different dependence on the effective mass. This discrepancy results in more than an order-of-magnitude deviation in emissivity, significantly impacting constraints on the KSVZ axion from the cooling observations of the Cassiopeia A neutron star. Furthermore, we examine uncertainties arising from neutron-star equations of state and their role in the discrepancy, finding that the large deviation persists regardless of the choice of equations of state.

*E-mail address: hama@hep-th.phys.s.u-tokyo.ac.jp

†E-mail address: natsumi@hep-th.phys.s.u-tokyo.ac.jp

‡E-mail address: zhengjm3@gmail.com

1 Introduction

Axion [1, 2]¹ is a pseudo-Nambu-Goldstone boson arising from the spontaneous breaking of the Peccei-Quinn symmetry [7, 8], originally proposed to resolve the strong CP problem. Its coupling to gluons via the quantum anomaly of the Peccei-Quinn symmetry induces an effective potential for the axion field, driving the system toward a CP-conserving vacuum. Several concrete realizations of this mechanism have been proposed in the literature, among which the KSVZ [9, 10] and DFSZ [11, 12] models are particularly well-known. In these models, the Peccei-Quinn symmetry-breaking scale is significantly higher than the electroweak scale. Since the couplings of axions are inversely proportional to this scale—a common feature of Nambu-Goldstone bosons—their interactions with Standard Model particles are extremely weak, and their mass, generated by the effective potential, is very small. These characteristics make experimental searches for axions highly challenging.

Observations of astrophysical objects place the most stringent constraints on axion models [13, 14]. In particular, SN1987A has provided the strongest limits over the years [15]. Axions, being extremely light and weakly coupled to ordinary matter, can freely escape from a core-collapse supernova once produced, whereas neutrinos remain trapped immediately after the collapse. Consequently, if too many axions are emitted, the supernova cools too rapidly, shortening the duration of neutrino emission compared to that observed for SN1987A. This observation thus restricts the axion-nucleon couplings. For example, a recent analysis constrains the axion decay constant to $f_a \gtrsim 4 \times 10^8$ GeV in the KSVZ model [16] (see also Refs. [17–24]).

A cooling constraint on axion-nucleon couplings can also be obtained from neutron star (NS) temperature observations [25–34]. Currently, the temperatures of approximately 60 NSs have been measured [35, 36], and the observed data generally align with the predictions of standard NS cooling theory [37–42].² Given this, NS temperature data can be used to constrain the existence of additional cooling sources, such as axions. Young NSs are particularly useful for this purpose, as the axion emission rate rapidly increases with temperature.

As it turns out, a young NS in the supernova remnant Cassiopeia A (Cas A) is potentially one of the most sensitive probes of axions. Since 2006, Chandra observations have revealed a steady decline in the surface temperature of the Cas A NS [53]. For a long time, this cooling trend was primarily observed in data taken in the GRADED mode of the ACIS detectors, which may suffer from pile-up effects [54]. More recently, observations in the FAINT mode—where pile-up effects are significantly reduced—have accumulated sufficient temporal coverage to confirm the rapid cooling of the Cas A NS at the 5σ level, assuming proper detector calibration [55]. The results from both observation modes are consistent and, when combined, suggest a cooling rate of $2.2 \pm 0.3\%$ over ten years, provided that the absorbing hydrogen column density is allowed to vary [56]. For a recent review on the Cas A NS cooling, see Ref. [57]. Notably, this cooling rate can be naturally explained within the standard NS cooling scenario if the neutron triplet superfluid transition has recently occurred [58–62]. In this case, enhanced neutrino emission

¹For a recent review on axions, see Refs.[3–6].

²However, some older NSs exhibit significantly higher temperatures than those predicted by the standard cooling scenario [43–49]. These observations can be explained by internal heating mechanisms [50–52], which are relevant only for old NSs and, in particular, do not affect the temperature of young NSs.

due to the breaking and reformation of neutron triplet Cooper pairs [63–65] in the NS core would accelerate the cooling rate, making it consistent with the observed rate. See also Refs. [66–80] for related discussions.

In Ref. [27], it was proposed that axion cooling could account for the observed cooling curve of the Cas A NS. Specifically, for the KSVZ axion, the analysis suggested that $C_n^2/f_a^2 \simeq 1.6 \times 10^{-19} \text{ GeV}^{-2}$ (C_n denotes the axion-neutron coupling, as defined in Eqs. (1) and (2) below) is consistent with the observations. However, Ref. [30] pointed out that such a small value of f_a would enhance axion emission from protons at earlier times—contribution not considered in Ref. [27]. As a result, the predicted temperature at the current age of the Cas A NS would be lower than observed, leading to a constraint on the axion decay constant: $f_a \gtrsim 5 \times 10^8 \text{ GeV}$ for the KSVZ model and $f_a \gtrsim 7 \times 10^8 \text{ GeV}$ for the DFSZ model with $\tan\beta = 10$,³ respectively. As a subsequent paper to Ref. [27], Ref. [32] revisited this analysis, shifting the focus from explaining the cooling curve via axion cooling in Ref. [27] to using the Cas A NS observations to constrain axion models. While the limit on the DFSZ axion in Ref. [32] was comparable to that in Ref. [30], the revised bound for the KSVZ axion in [32] differed significantly, yielding $f_a > 3 \times 10^7 \text{ GeV}$.

The purpose of this paper is to identify the source of this discrepancy. We find that the formula for axion emissivity from singlet proton Cooper pairs used in Ref. [32] differs in its dependence on the effective mass from those in other works [28, 30, 33, 81], leading to a significant difference in the total axion emission rate for the KSVZ axion. In Sec. 2, we review the calculation of emissivity for this process, followed by an analysis in Sec. 3 of how the difference in effective mass dependence affects the results. In Sec. 4, we examine the uncertainty in axion emissivity due to the NS equation of state (EOS), which influences the calculation through the effective mass, Fermi momentum, and pairing energy gap. We also discuss the significance of this uncertainty on the discrepancy. Finally, Sec. 5 presents our conclusions.

2 Axion emission from singlet Cooper pairs

We begin by calculating the emissivity of axions from singlet proton Cooper pairs, a process known as pair-breaking and formation (PBF). In Ref. [81], this emissivity was derived using a transport equation and by evaluating the correlation functions of nucleon axial currents. Here, we revisit the calculation using the method of the Bogolyubov–Valatin transformations [82–84].

The axion-nucleon interactions have the form

$$\mathcal{L}_{aNN} = \sum_{N=p,n} \frac{C_N}{2f_a} \bar{N} \gamma^\mu \gamma_5 N \partial_\mu a, \quad (1)$$

where C_N ($N = p, n$) are the axion-nucleon couplings, whose size depends on axion models. For the KSVZ axion, the couplings are [85]

$$C_p = -0.47(3), \quad C_n = -0.02(3). \quad (2)$$

Notice that the axion-neutron coupling C_n is highly suppressed in this model.

³ $\tan\beta$ is the ratio of the vacuum expectation values of the two Higgs doublets in the DFSZ axion model.

To avoid unnecessary complications with subscripts, we perform our calculations exclusively for proton pairs. The results for neutrons can be easily obtained by replacing the corresponding quantities with those for neutrons.

In the presence of singlet Cooper pairs, the annihilation operators of quasi-particles on the paired ground state with momentum \mathbf{p} and spin s , $\hat{\alpha}_{\mathbf{p},s}$, are related to those in the non-interacting Hamiltonian, $\hat{a}_{\mathbf{p},s}$, as [82–84]

$$\begin{aligned}\hat{\alpha}_{\mathbf{p},+} &= u_p \hat{a}_{\mathbf{p},+} - v_p \hat{a}_{-\mathbf{p},-}^\dagger, \\ \hat{\alpha}_{\mathbf{p},-} &= u_p \hat{a}_{\mathbf{p},-} + v_p \hat{a}_{-\mathbf{p},+}^\dagger,\end{aligned}\tag{3}$$

with

$$u_p = \frac{1}{\sqrt{2}} \left(1 + \frac{\eta_p}{\sqrt{\eta_p^2 + \Delta^2}} \right)^{\frac{1}{2}}, \quad v_p = \frac{1}{\sqrt{2}} \left(1 - \frac{\eta_p}{\sqrt{\eta_p^2 + \Delta^2}} \right)^{\frac{1}{2}},\tag{4}$$

where Δ is the energy gap, and near the Fermi surface η_p has the form

$$\eta_p \simeq v_F(p - p_F),\tag{5}$$

where p_F and v_F are the Fermi momentum and velocity, respectively, and $p \equiv |\mathbf{p}|$. The energy of a quasi-particle is given by

$$\epsilon_p = \sqrt{\eta_p^2 + \Delta^2}.\tag{6}$$

The matrix elements of the proton field operator between the ground state $|\Omega\rangle$ and the one-quasi-particle states $|\mathbf{p}, s\rangle$ are⁴

$$\langle \Omega | p(x) | \mathbf{p}, s \rangle = U_{ss'}(p) \begin{pmatrix} \sqrt{p_0 + m^*} \xi_{s'} \\ \sqrt{p_0 - m^*} \hat{\mathbf{p}} \cdot \boldsymbol{\sigma} \xi_{s'} \end{pmatrix} e^{-ip \cdot x},\tag{7}$$

$$\langle \Omega | \bar{p}(x) | \mathbf{p}, s \rangle = \left(\sqrt{p_0 + m^*} \xi_{s'}^\dagger, \sqrt{p_0 - m^*} \xi_{s'}^\dagger \hat{\mathbf{p}} \cdot \boldsymbol{\sigma} \right) V_{s's}(p) e^{ip \cdot x},\tag{8}$$

where ξ_s denotes a two-component spinor, $\hat{\mathbf{p}} \equiv \mathbf{p}/|\mathbf{p}|$, σ^i ($i = 1, 2, 3$) are the Pauli matrices, the effective mass $m^* = p_F/v_F$, $p^0 \simeq m^* + \mathbf{p}^2/(2m^*)$, and

$$U_{ss'}(p) = \begin{pmatrix} u_p & 0 \\ 0 & u_p \end{pmatrix}, \quad V_{ss'}(p) = \begin{pmatrix} 0 & v_p \\ -v_p & 0 \end{pmatrix}.\tag{9}$$

As it turns out, the emissivity of axions in the singlet PBF process vanishes in the non-relativistic limit, $v_F \rightarrow 0$ [81].⁵ We therefore keep $\mathcal{O}(v_F)$ terms in the amplitude calculation. The emissivity is given by

$$\begin{aligned}\epsilon_a^S &= \frac{1}{2} \int \frac{d^3\mathbf{p}}{(2\pi)^3 2p_0} \frac{d^3\mathbf{p}'}{(2\pi)^3 2p'_0} \frac{d^3\mathbf{q}}{(2\pi)^3 2q_0} q_0 f(p) f(p') \\ &\quad \times (2\pi)^4 \delta^3(\mathbf{p} + \mathbf{p}' - \mathbf{q}) \delta(\epsilon_p + \epsilon_{p'} - q_0) \sum_{s,s'} |\mathcal{M}|^2,\end{aligned}\tag{10}$$

⁴We use the Dirac representation for the four-component spinor coefficient functions.

⁵This is the same as in the case of the neutrino PBF emission from singlet Cooper pairs via the nucleon axial current [86].

where q , p , and p' are the four-momenta of axion and quasi-particles, respectively, $f(p)$ denotes the Fermi-Dirac distribution function, and

$$i\mathcal{M} = -\frac{C_p}{2f_a} q_\mu \langle \Omega | \bar{p} \gamma^\mu \gamma_5 p | \mathbf{p}, s; \mathbf{p}', s' \rangle . \quad (11)$$

The overall factor $1/2$ in Eq. (10) is to avoid double count in the momentum integral of quasi-particles. At $\mathcal{O}(v_F^2)$, the square of the matrix element is obtained as

$$\begin{aligned} \sum_{s,s'} |\mathcal{M}|^2 = \frac{C_p^2}{2f_a^2} (2m^*)^2 & \left[q_0^2 \frac{(\mathbf{p} - \mathbf{p}')^2}{(2m^*)^2} (u_p v_{p'} + u_{p'} v_p)^2 + \mathbf{q}^2 (u_p v_{p'} - u_{p'} v_p)^2 \right. \\ & \left. - 2q_0 \mathbf{q} \cdot \frac{(\mathbf{p} - \mathbf{p}')}{2m^*} (u_p^2 v_{p'}^2 - u_{p'}^2 v_p^2) \right] . \end{aligned} \quad (12)$$

The first, second, and third terms in the square bracket originate from the temporal, spatial, and temporal-spatial mixed parts,⁶ respectively—all of these contribute at the same order in v_F [88], as we see below.

We can readily perform the integral (10) with respect to the axion momentum \mathbf{q} , eliminating the momentum delta function with the momentum conservation $\mathbf{q} = \mathbf{p} + \mathbf{p}'$. For quasi-particle momenta, we note that for PBF emission in NSs, only narrow regions of momentum near the Fermi surface contribute to the integral. Hence, we can take $|\mathbf{p}| = |\mathbf{p}'| = p_F$ in any smooth functions in the integrand. In particular, we can set

$$d^3 \mathbf{p}, d^3 \mathbf{p}' \rightarrow p_F^2 dp d\Omega_p, p_F^2 dp' d\Omega_{p'} , \quad (13)$$

where $p = |\mathbf{p}|$, $p' = |\mathbf{p}'|$, and $d\Omega_p, d\Omega_{p'}$ are solid-angle elements. One of the angular integrals converts to a factor of 4π because of the rotational invariance of the system. For the other one, the axial symmetry yields a factor of 2π , and the remaining integral removes the delta function for energy conservation. Notice that since the axion energy in the PBF process is comparable to the size of the pairing gap, $\Delta \ll p_F$ implies $|\mathbf{q}| \ll |\mathbf{p}|, |\mathbf{p}'|$, and thus $\mathbf{p}' \simeq -\mathbf{p}$; only this anti-parallel region contributes to the angular integral in Eq. (10). From the kinematic condition, it follows that the discrepancy in the size of \mathbf{p} and \mathbf{p}' is restricted in the range $|p - p'| \leq \epsilon_p + \epsilon_{p'}$.

We are now left with the integral with respect to p and p' . To simplify the expression, let us introduce the following dimensionless variables:

$$x^{(\prime)} \equiv \frac{v_F(p^{(\prime)} - p_F)}{T} , \quad y \equiv \frac{\Delta}{T} , \quad z^{(\prime)} \equiv \frac{\epsilon_{p^{(\prime)}}}{T} , \quad (14)$$

with T the local temperature. We change the integral variables from p, p' to x, x' , with the integral range restricted to

$$|x - x'| \leq v_F(z + z') . \quad (15)$$

⁶In earlier studies [86] on singlet PBF neutrino emission, the temporal-spatial mixed part of the squared matrix element of the axial-current was ignored, and this result was adopted in NSCool [87] for numerical simulations. We have verified that when applied to neutrino emission via the weak interaction, our evaluation of the squared axial-current matrix element in Eq. (12) is consistent with the result in Ref. [88], after accounting for medium corrections that suppress the vector current contribution.

We can therefore regard $x - x'$ as an $\mathcal{O}(v_F)$ quantity. The terms in the square bracket in Eq. (12) are now computed as

$$q_0^2 \frac{(\mathbf{p} - \mathbf{p}')^2}{(2m^*)^2} (u_p v_{p'} + u_{p'} v_p)^2 = 4v_F^2 T^2 y^2, \quad (16)$$

$$\mathbf{q}^2 (u_p v_{p'} - u_{p'} v_p)^2 = T^2 \frac{y^2}{z^2} (x - x')^2, \quad (17)$$

$$-2q_0 \mathbf{q} \cdot \frac{(\mathbf{p} - \mathbf{p}')}{2m^*} (u_p^2 v_{p'}^2 - u_{p'}^2 v_p^2) = -2T^2 \frac{y^2}{z^2} (x - x')^2, \quad (18)$$

at the leading order in the v_F expansion. The integral (10) is then expressed as

$$\epsilon_a^S = \frac{C_p^2}{16\pi^3 f_a^2} m^{*2} T^5 y^2 \int_0^\infty dx \frac{z}{(e^z + 1)^2} \int_{-2v_F z}^{2v_F z} d\xi \left[4v_F^2 + \frac{\xi^2}{z^2} - 2\frac{\xi^2}{z^2} \right], \quad (19)$$

where we set $\xi = x - x'$ and extend the upper limit of the x integral to infinity since this integral is rapidly convergent for large x . After performing the ξ integral, we finally obtain

$$\epsilon_a^S = \frac{2}{3} \cdot \frac{C_p^2}{\pi f_a^2} \cdot \left(\frac{m^* p_F}{\pi^2} \right) v_F^2 T^5 F_s \left(\frac{\Delta}{T} \right), \quad (20)$$

where

$$F_s(y) \equiv y^2 \int_0^\infty dx \frac{z^2}{(e^z + 1)^2}. \quad (21)$$

3 Comparison of previous calculations

By noting

$$I_{aN}^S = F_s \left(\frac{\Delta_N^S(T)}{T} \right), \quad (22)$$

we find that the result obtained in the previous section is consistent with those in Refs. [28, 81], which was used in the analysis in Ref. [30]. A useful fit function for the function (21) is given in Ref. [28]:

$$F_s(z) = (az^2 + cz^4) \sqrt{1 + fze^{-\sqrt{4z^2 + h^2} + h}}, \quad (23)$$

where $a = 0.158151$, $c = 0.543166$, $h = 0.0535359$, and $f = \pi/4c^2 = 2.6621$. This fit was used in the numerical computation in Ref. [30]. Numerically, the emissivity (20) is given by

$$\begin{aligned} \epsilon_a^S \simeq 1.14 \times 10^{21} \times \left(\frac{C_N}{2} \right)^2 \left(\frac{10^{10} \text{ GeV}}{f_a} \right)^2 \left(\frac{m_N^*}{m_N} \right)^2 \left(\frac{v_{F,N}}{c} \right)^3 \left(\frac{T}{10^9 \text{ K}} \right)^5 \\ \times F_s \left(\frac{\Delta_N^S(T)}{T} \right) \text{ erg} \cdot \text{cm}^{-3} \cdot \text{s}^{-1}, \end{aligned} \quad (24)$$

which is again consistent with the expression given in Ref. [81].

As seen in the case of the neutrino PBF emission via the axial current [88], we expect a certain amount of medium corrections to the axion-nucleon interactions through the vertex and wave-function renormalization. In Ref. [33], this correction is estimated by a correction factor

$$\gamma = \left[1 + \frac{1}{3} \left(\frac{m_N^*}{m_N} \right) \left(\frac{p_{F,n}}{1.68 \text{ fm}^{-1}} \right) \right]^{-1}. \quad (25)$$

This can lead to an $\mathcal{O}(10)\%$ reduction in the emissivity. Besides this factor and an overall numerical factor of $\simeq 1.5$, the semi-analytical expression shown in Ref. [33] is consistent with Eq. (24).

On the other hand, Ref. [32] shows a semi-analytic formula for the singlet axion PBF emissivity for proton⁷

$$Q_{pa}^{\text{PBF}} = 1.55 \times 10^{40} g_{app}^2 \left(\frac{m_p^*}{m_p} \right)^2 \left(\frac{T}{10^9 \text{ K}} \right)^5 \left(\frac{p_{F,p}}{m_p c} \right)^3 \frac{6}{7} F_2 \left(\frac{T}{T_{cp}} \right) \frac{\text{erg}}{\text{cm}^3 \cdot \text{s}}, \quad (28)$$

where $g_{app} = C_p m_p / f_a$ and

$$F_2(T/T_c) = \frac{\Delta_N^2}{T^2} \int_0^\infty dx \frac{z^2}{(\exp z + 1)^2}, \quad (29)$$

with $z = \sqrt{x^2 + \Delta_N^2/T^2}$; *i.e.*, $F_2 = F_s$. We observe that, apart from an overall factor, this expression exhibits a different dependence on the effective mass compared to Eq. (20); the emissivity in Eq. (28) is proportional to $(m_p^*)^2 p_{F,p}^3$,⁸ whereas Eq. (20) is proportional to $p_{F,p}^3/m_p^*$. We are unable to determine the origin of this discrepancy since the derivation of the axion emissivity was not provided in Ref. [32]. Given that the effective mass in the NS core can be significantly smaller than that in the vacuum, this difference could lead to a substantial deviation in the emissivity.

To illustrate this, in Fig. 1, we show the ratio m_N^*/m_N as a function of the distance r from the center of the NS, where the solid and dashed lines are for proton and neutron, respectively. The black and red lines correspond to NSs with a mass of $1.4M_\odot$, constructed using the APR EOS [89] (adopted in Ref. [30]) and the BSK21 EOS [90, 92] (adopted in Ref. [32]). We also present effective masses for more recent EOSs provided in Ref. [91].⁹

⁷This is taken from the journal version and arXiv v3 of Ref. [32]. Different expressions are presented in other arXiv versions; in v1,

$$Q_{pa}^{\text{PBF}} = 1.55 \times 10^{40} g_{app}^2 \frac{p_{F,p}}{m_p^*} \left(\frac{m_p^*}{m_p} \right)^2 \left(\frac{T}{10^9 \text{ K}} \right)^5 \left(\frac{p_{F,p}}{m_p c} \right)^2 \left[\left(\frac{m_p^*}{m_p} \right)^2 + \frac{11}{42} \right] F_2 \left(\frac{T}{T_{cp}} \right) \frac{\text{erg}}{\text{cm}^3 \cdot \text{s}}, \quad (26)$$

and in v2

$$Q_{pa}^{\text{PBF}} = 1.55 \times 10^{40} g_{app}^2 \frac{p_{F,p}}{m_p^*} \left(\frac{m_p^*}{m_p} \right)^2 \left(\frac{T}{10^9 \text{ K}} \right)^5 \left(\frac{p_{F,p}}{m_p c} \right)^2 \frac{6}{7} F_2 \left(\frac{T}{T_{cp}} \right) \frac{\text{erg}}{\text{cm}^3 \cdot \text{s}}. \quad (27)$$

⁸The emissivities in arXiv v1 and v2 of [32] (Eq. (26) and Eq. (27), respectively) also exhibit different dependencies on the effective mass.

⁹For density above 10^6 g/cm^3 corresponding to the core and the inner crust of a NS, we obtain the BSK EOSs from the fitting programs provided in [93]. For lower densities in the outer crust, the EOSs are read from [91, 92]. To build the NS profile, we modified and ran the Tolman-Oppenheimer-Volkov equation solver and the main program in the NSCool [87] package.

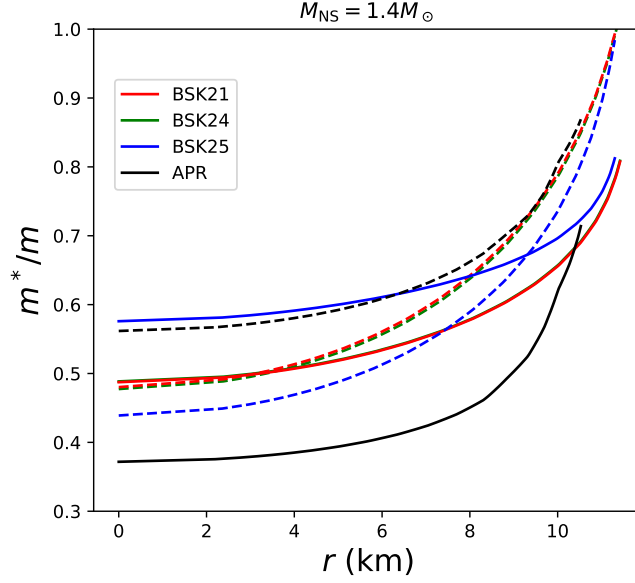


Figure 1: The ratio m_N^*/m_N as functions of the distance from the center of the NS, r . The solid and dashed lines are for proton and neutron, respectively. The black, red, green, and blue lines correspond to NSs with a mass of $1.4M_\odot$, constructed using the APR EOS [89], the BSK21 EOS [90], the BSK24 EOS [91], and the BSK25 EOS [91], respectively.

The results for the BSK24 and BSK25 EOSs are shown in green and blue, respectively. Notably, the BSK24 result (green) is almost identical to that of BSK21 (red), and this similarity persists in the following analysis. We do not include results for BSK22 and BSK26 [91]. The BSK22 EOS allows the direct URCA process to operate in a NS with a mass $\gtrsim 1.151M_\odot$ [91], which would render the temperature of Cas A—estimated to have a mass of $1.55 \pm 0.25M_\odot$ [56]—too low at the time of observation. On the other hand, the BSK26 EOS is inconsistent with the mass-radius measurements of PSR J0030 and PSR J0740 based on *NICER* data [33, 94].

As can be seen in Fig. 1, in the core region m_p^*/m_p can be as low as $\simeq 0.5$. Consequently, the factor of $(m_p^*)^3$ leads to almost an order-of-magnitude difference in emissivity between Ref. [30] and Ref. [32].

We compare our results with the previous calculations in Fig. 2. Figures 2a and 2b show the axion emissivity, ϵ_a^S , and the emission rate in a spherical shell, $4\pi r^2 \epsilon_a^S$, respectively, as functions of the distance from the center of a $1.4M_\odot$ NS constructed with the BSK21 EOS and the CCDK proton pairing gap model [95]. We set $T = 10^9$ K and $C_p/f_a = 10^{-10}$ GeV $^{-1}$. The black solid line represents our result, as described in Sec. 2, which is consistent with those used in Refs. [28, 30, 81]. The blue solid (dashed) line corresponds to the semi-analytical expression in Ref. [33] with (without) the correction factor γ in Eq. (25). The red solid line shows the semi-analytical result from the journal version and arXiv v3 of Ref. [32]. It turns out that our result, given in Eq. (20), agrees well with that of Ref. [33]. In particular, the effect of the medium correction is small, indicating that the theoretical uncertainty in our calculation is well controlled. In contrast, the emissivity in Ref. [32] is found to be significantly lower than the others. This discrepancy

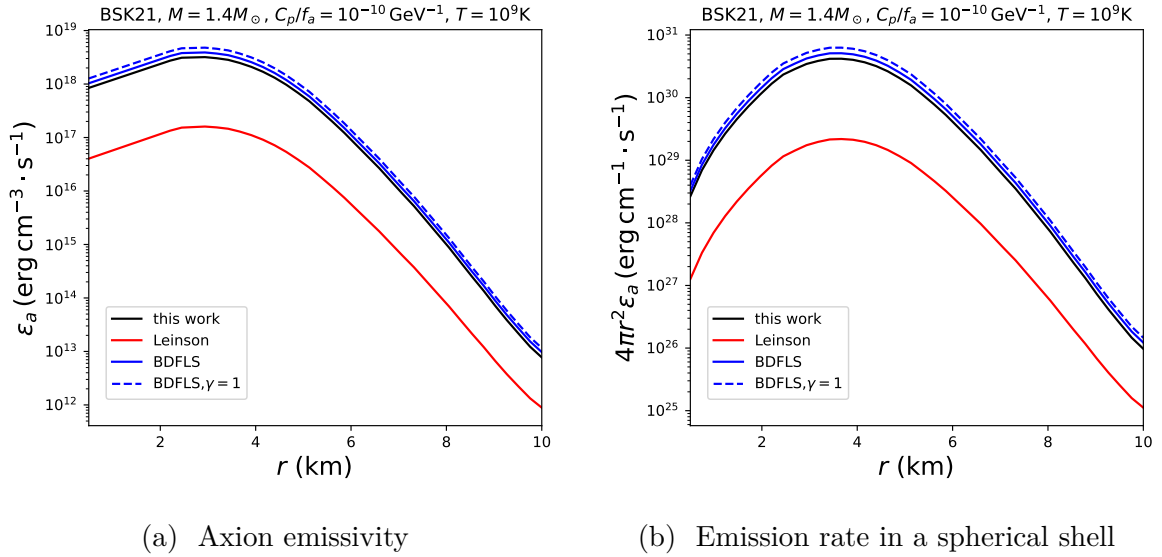


Figure 2: a) The axion emissivity and b) the emission rate in a spherical shell from proton singlet pairings as functions of the distance from the center of a $1.4M_{\odot}$ NS constructed with the BSK21 EOS and the CCDK proton pairing gap model [95], where we set $T = 10^9$ K and $C_p/f_a = 10^{-10}$ GeV $^{-1}$. The black solid, red solid, blue solid, and blue dashed lines correspond to Eq. (20), Eq. (28), the expression given in Ref. [33], and that in Ref. [33] with $\gamma = 1$, respectively.

is attributed to the difference in the dependence on the effective mass.

As discussed in Ref. [30], for the KSVZ axion, the proton PBF is the dominant axion emission process because of the suppressed axion-neutron coupling (see Eq. (2)). As a result, a lower emissivity of the proton PBF leads to a weaker limit on the axion decay constant. Indeed, the axion emission luminosity of the proton PBF shown in Ref. [32] is significantly lower than that in Ref. [30]. This indicates that the weaker constraint on the KSVZ axion reported in Ref. [32] stems from an underestimated proton PBF emissivity, which in turn arises from an incorrect effective mass dependence in the axion emissivity formula used in Ref. [32].

4 EOS dependence

As evident from Eq. (20), the emissivity of axions depends not only on the effective mass but also on the Fermi momentum and the pairing gap, both of which are influenced by the choice of NS EOS, as shown in Fig. 3. In Fig. 3a, we show the proton Fermi momenta $p_{F,p}$ as a function of the distance from the NS center, computed for different EOSs. For $r \lesssim 9$ km, the proton Fermi momenta—and consequently, the proton densities—exhibit only minor variations among the BSK EOSs, whereas those for the APR EOS are $\sim 10\%$ higher than the others. On the other hand, in the lower density region at $r \gtrsim 9$ km, the proton Fermi momentum for the APR EOS is much lower than that for the BSK21, 24, and 25 EOSs. It is, however, worth noting that axion emission in this region is highly suppressed compared to the NS core, as can be seen in Fig. 4 below.

Fig. 3b shows the profile of the proton singlet pairing gap Δ_p^S at $T = 0$, obtained

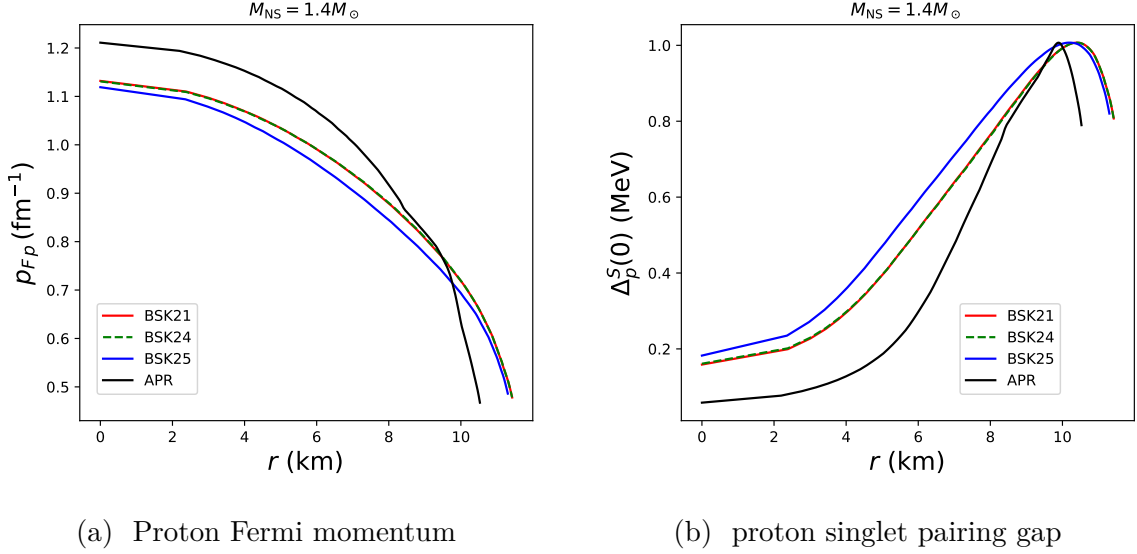


Figure 3: a) The proton Fermi momentum as a function of the distance from the NS center; b) The proton singlet pairing gap profile at $T = 0$ obtained with the CCDK gap model.

with the CCDK gap model for various EOSs. The variations in Δ_p^S across different EOSs originate from the dependence of the pairing gap on $p_{F,p}$. In the core region, the pairing gap for the APR EOS differs by an $\mathcal{O}(1)$ factor from those for BSK EOSs, which significantly alters the emissivity due to its exponential dependence on Δ_p^S , as seen in Eq. (21).

This effect is illustrated in Fig. 4, where we plot the axion emissivity in Fig. 4a and the axion emission rate within a spherical shell in Fig. 4b, both from proton singlet pairings, as functions of the distance from the center of a $1.4M_{\odot}$ NS constructed with various EOSs. We use the CCDK proton pairing gap model [95] and set $T = 10^9$ K and $C_p/f_a = 10^{-10} \text{ GeV}^{-1}$. For the APR EOS, plotted with the black line, protons are unpaired at $r \lesssim 4$ km because of the small proton pairing gap in this region, as shown in Fig. 3b. As a result, the proton PBF process is inactive in this region for the APR EOS.

In Fig. 5, we present the ratios of proton-PBF axion emissivities obtained from expressions in the literature to the result re-derived in this work, plotted as functions of the distance from the center of a $1.4M_{\odot}$ NS constructed with various EOSs. In this figure, ϵ_a is calculated using the semi-analytical expression in Eq. (24), while ϵ_a^L in Fig. 5a is obtained from Eq. (28) adopted from Ref. [32] and ϵ_a^B in Fig. 5b is calculated from Eq. (S8) in Ref. [33] including the medium correction factor γ . Figure 5a shows that the ratio ϵ_a^L/ϵ_a is much smaller than unity and highly sensitive to the choice of the EOS due to the additional $(m_p^*/m_p)^3$ dependence in Eq. (28) compared to Eq. (24). As we have seen in Fig. 1, the proton effective mass can be considerably lower than its vacuum mass and varies significantly among different EOSs, leading to a discrepancy between the emissivities obtained in Ref. [32] and those in Ref. [30] by more than an order of magnitude, with large uncertainties arising from the choice of EOSs. On the other hand, as shown in Fig. 5b, the difference between ϵ_a^B and ϵ_a is just an $\mathcal{O}(10)\%$ level and exhibits much smaller variations across different EOSs. This is because the EOS dependence in the ratio

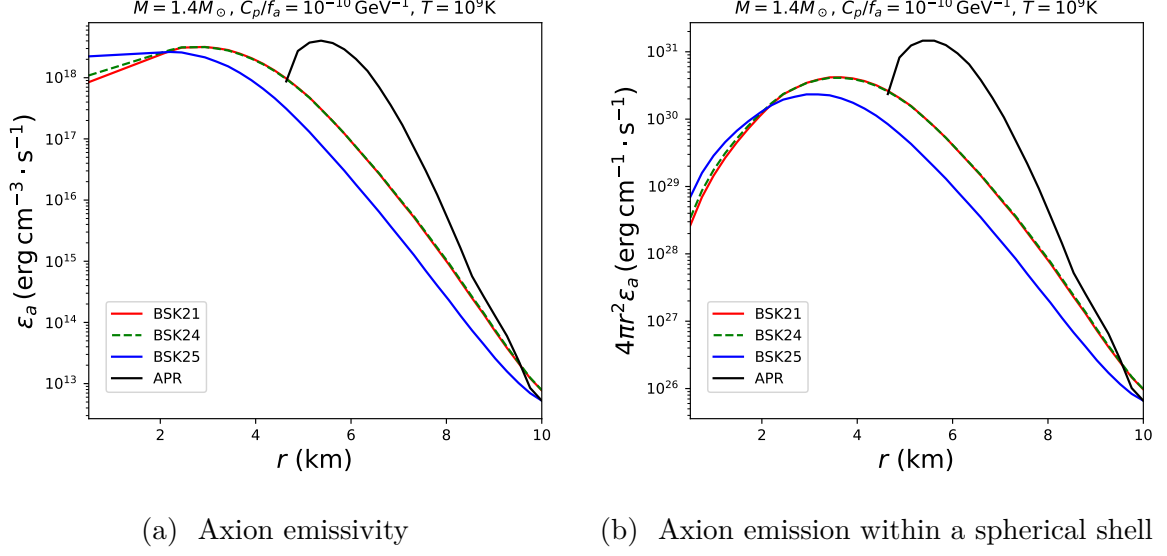


Figure 4: a) The axion emissivity and b) the axion emission rate in a spherical shell from proton singlet pairings as functions of the distance from the center of a $1.4M_{\odot}$ NS constructed with various EOSs, where we use the CCDK proton pairing gap model [95] and set $T = 10^9$ K and $C_p/f_a = 10^{-10}$ GeV $^{-1}$.

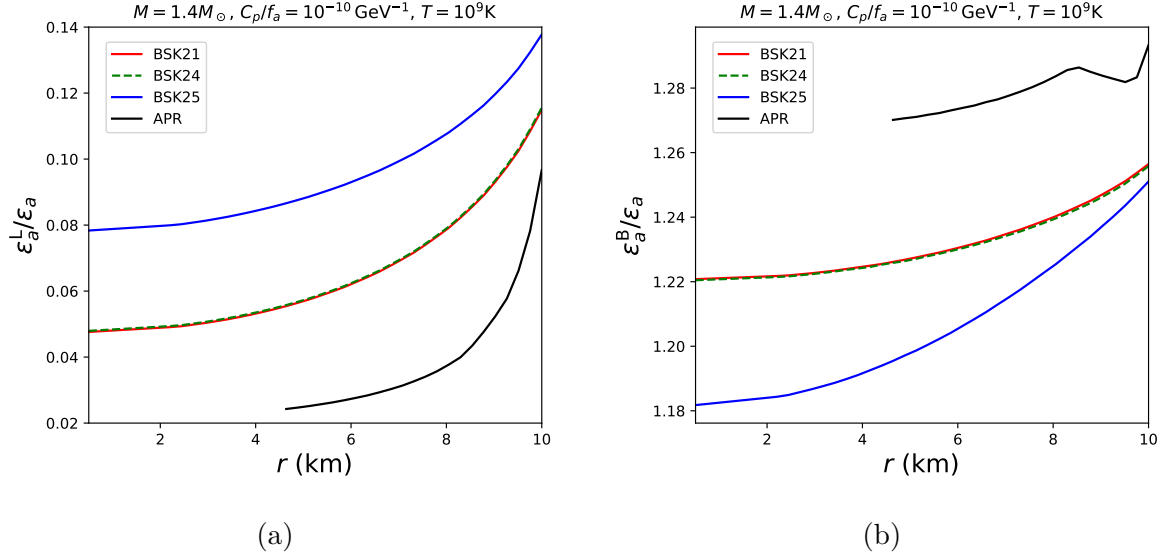


Figure 5: The ratio of emissivities calculated using a) Eq. (28) from Ref. [32] and b) expression in Ref. [33] with the medium correction factor, to our result in Eq. (24), as functions of the distance from the center of a $1.4M_{\odot}$ NS constructed with various EOSs. Other parameters are the same as those in Fig. 4.

ϵ_a^B/ϵ_a enters only through the medium correction factor γ in ϵ_a^B , as described in Eq. (25), which is far less sensitive to the EOS than the $(m_p^*/m_p)^3$ factor in ϵ_a^L/ϵ_a .

5 Conclusion

In this study, we have re-derived the emissivity of axions from singlet proton Cooper pairs in NSs and compared it with previous results in the literature. Our re-derived expression, which was used in Ref. [30] and consistent with those in Refs. [28, 81], is in close agreement with the results in Ref. [33] but differs significantly from those in Ref. [32]. This discrepancy, combined with different choices of the NS EOS, can explain the differences in the proton-PBF emissivities of the KSVZ axion for the Cas A NS in Refs. [30] and Ref. [32]. We have also investigated the impact of different EOS choices on axion emissivity and found that the large discrepancy persists regardless of the choice of EOSs.

As shown in Fig. 1, the effective mass of not only protons but also neutrons depends on the choice of EOS. This, together with the EOS dependence of the Fermi momentum and pairing gaps of neutrons, also affects the total axion emissivity as well as that of neutrinos. All of these factors collectively affect the constraints on axion-nucleon couplings derived from the Cas A NS. We will update these constraints by systematically incorporating EOS dependence and utilizing the latest data of the temperature observations of the Cas A NS in future work.

Acknowledgments

We thank Andrew J. Long for useful correspondence. This work was supported by JSPS KAKENHI Grant Numbers 24H02244 (KH), 24K07041 (KH), and 21K13916 (NN).

References

- [1] S. Weinberg, *A New Light Boson?*, [Phys. Rev. Lett.](#) **40** (1978) 223–226.
- [2] F. Wilczek, *Problem of Strong P and T Invariance in the Presence of Instantons*, [Phys. Rev. Lett.](#) **40** (1978) 279–282.
- [3] L. Di Luzio, M. Giannotti, E. Nardi, and L. Visinelli, *The landscape of QCD axion models*, [Phys. Rept.](#) **870** (2020) 1–117 [[arXiv:2003.01100](#)].
- [4] K. Choi, S. H. Im, and C. Sub Shin, *Recent Progress in the Physics of Axions and Axion-Like Particles*, [Ann. Rev. Nucl. Part. Sci.](#) **71** (2021) 225–252 [[arXiv:2012.05029](#)].
- [5] C. Antel *et al.*, *Feebly-interacting particles: FIPs 2022 Workshop Report*, [Eur. Phys. J. C](#) **83** (2023) 1122 [[arXiv:2305.01715](#)].
- [6] **Particle Data Group** Collaboration, *Review of particle physics*, [Phys. Rev. D](#) **110** (2024) 030001.

- [7] R. D. Peccei and H. R. Quinn, *CP Conservation in the Presence of Instantons*, [Phys. Rev. Lett. **38** \(1977\) 1440–1443](#).
- [8] R. D. Peccei and H. R. Quinn, *Constraints Imposed by CP Conservation in the Presence of Instantons*, [Phys. Rev. D **16** \(1977\) 1791–1797](#).
- [9] J. E. Kim, *Weak Interaction Singlet and Strong CP Invariance*, [Phys. Rev. Lett. **43** \(1979\) 103](#).
- [10] M. A. Shifman, A. I. Vainshtein, and V. I. Zakharov, *Can Confinement Ensure Natural CP Invariance of Strong Interactions?*, [Nucl. Phys. B **166** \(1980\) 493–506](#).
- [11] A. R. Zhitnitsky, *On Possible Suppression of the Axion Hadron Interactions. (In Russian)*, [Sov. J. Nucl. Phys. **31** \(1980\) 260](#).
- [12] M. Dine, W. Fischler, and M. Srednicki, *A Simple Solution to the Strong CP Problem with a Harmless Axion*, [Phys. Lett. B **104** \(1981\) 199–202](#).
- [13] A. Caputo and G. Raffelt, *Astrophysical Axion Bounds: The 2024 Edition*, [PoS COSMICWISPers \(2024\) 041 \[arXiv:2401.13728\]](#).
- [14] P. Carenza, M. Giannotti, J. Isern, A. Mirizzi, and O. Straniero, *Axion Astrophysics*, [arXiv:2411.02492](#) (2024).
- [15] G. G. Raffelt, *Astrophysical axion bounds*, [Lect. Notes Phys. **741** \(2008\) 51–71 \[hep-ph/0611350\]](#).
- [16] P. Carenza, *et al.*, *Improved axion emissivity from a supernova via nucleon-nucleon bremsstrahlung*, [JCAP **10** \(2019\) 016 \[arXiv:1906.11844\]](#). [Erratum: JCAP 05, E01 (2020)].
- [17] J. Martin Camalich, M. Pospelov, P. N. H. Vuong, R. Ziegler, and J. Zupan, *Quark Flavor Phenomenology of the QCD Axion*, [Phys. Rev. D **102** \(2020\) 015023 \[arXiv:2002.04623\]](#).
- [18] P. Carenza, B. Fore, M. Giannotti, A. Mirizzi, and S. Reddy, *Enhanced Supernova Axion Emission and its Implications*, [Phys. Rev. Lett. **126** \(2021\) 071102 \[arXiv:2010.02943\]](#).
- [19] J. M. Camalich, J. Terol-Calvo, L. Tolos, and R. Ziegler, *Supernova Constraints on Dark Flavored Sectors*, [Phys. Rev. D **103** \(2021\) L121301 \[arXiv:2012.11632\]](#).
- [20] K. Choi, H. J. Kim, H. Seong, and C. S. Shin, *Axion emission from supernova with axion-pion-nucleon contact interaction*, [JHEP **02** \(2022\) 143 \[arXiv:2110.01972\]](#).
- [21] T. Vonk, F.-K. Guo, and U.-G. Meißner, *Pion axioproduction: The Δ resonance contribution*, [Phys. Rev. D **105** \(2022\) 054029 \[arXiv:2202.00268\]](#).
- [22] S.-Y. Ho, J. Kim, P. Ko, and J.-h. Park, *Supernova axion emissivity with $\Delta(1232)$ resonance in heavy baryon chiral perturbation theory*, [Phys. Rev. D **107** \(2023\) 075002 \[arXiv:2212.01155\]](#).

- [23] A. Lella, *et al.*, *Getting the most on supernova axions*, *Phys. Rev. D* **109** (2024) 023001 [[arXiv:2306.01048](#)].
- [24] M. Cavan-Piton, D. Guadagnoli, M. Oertel, H. Seong, and L. Vittorio, *Axion Emission from Strange Matter in Core-Collapse SNe*, *Phys. Rev. Lett.* **133** (2024) 121002 [[arXiv:2401.10979](#)].
- [25] N. Iwamoto, *Axion Emission from Neutron Stars*, *Phys. Rev. Lett.* **53** (1984) 1198–1201.
- [26] H. Umeda, N. Iwamoto, S. Tsuruta, L. Qin, and K. Nomoto in *Workshop on Neutron Stars and Pulsars: Thirty Years After the Discovery*. 1997. [astro-ph/9806337](#).
- [27] L. B. Leinson, *Axion mass limit from observations of the neutron star in Cassiopeia A*, *JCAP* **08** (2014) 031 [[arXiv:1405.6873](#)].
- [28] A. Sedrakian, *Axion cooling of neutron stars*, *Phys. Rev. D* **93** (2016) 065044 [[arXiv:1512.07828](#)].
- [29] A. Paul, D. Majumdar, and K. Prasad Modak, *Neutron star cooling via axion emission by nucleon–nucleon axion bremsstrahlung*, *Pramana* **92** (2019) 44 [[arXiv:1801.07928](#)].
- [30] K. Hamaguchi, N. Nagata, K. Yanagi, and J. Zheng, *Limit on the Axion Decay Constant from the Cooling Neutron Star in Cassiopeia A*, *Phys. Rev. D* **98** (2018) 103015 [[arXiv:1806.07151](#)].
- [31] M. V. Beznogov, E. Rrapaj, D. Page, and S. Reddy, *Constraints on Axion-like Particles and Nucleon Pairing in Dense Matter from the Hot Neutron Star in HESS J1731-347*, *Phys. Rev. C* **98** (2018) 035802 [[arXiv:1806.07991](#)].
- [32] L. B. Leinson, *Impact of axions on the Cassiopeia A neutron star cooling*, *JCAP* **09** (2021) 001 [[arXiv:2105.14745](#)].
- [33] M. Buschmann, C. Dessert, J. W. Foster, A. J. Long, and B. R. Safdi, *Upper Limit on the QCD Axion Mass from Isolated Neutron Star Cooling*, *Phys. Rev. Lett.* **128** (2022) 091102 [[arXiv:2111.09892](#)].
- [34] A. Gómez-Bañón, K. Bartnick, K. Springmann, and J. A. Pons, *Constraining Light QCD Axions with Isolated Neutron Star Cooling*, *Phys. Rev. Lett.* **133** (2024) 251002 [[arXiv:2408.07740](#)].
- [35] A. Y. Potekhin, D. A. Zyuzin, D. G. Yakovlev, M. V. Beznogov, and Y. A. Shibano, *Thermal luminosities of cooling neutron stars*, *Mon. Not. Roy. Astron. Soc.* **496** (2020) 5052–5071 [[arXiv:2006.15004](#)].
- [36] *Cooling neutron stars*, <http://www.ioffe.ru/astro/NSG/thermal/cooldat.html>.
- [37] D. G. Yakovlev, K. P. Levenfish, and Y. A. Shibano, *Cooling neutron stars and superfluidity in their interiors*, *Phys. Usp.* **42** (1999) 737–778 [[astro-ph/9906456](#)].

- [38] D. G. Yakovlev, A. D. Kaminker, O. Y. Gnedin, and P. Haensel, *Neutrino emission from neutron stars*, *Phys. Rept.* **354** (2001) 1 [[astro-ph/0012122](#)].
- [39] D. G. Yakovlev and C. J. Pethick, *Neutron star cooling*, *Ann. Rev. Astron. Astrophys.* **42** (2004) 169–210 [[astro-ph/0402143](#)].
- [40] D. Page, J. M. Lattimer, M. Prakash, and A. W. Steiner, *Minimal cooling of neutron stars: A New paradigm*, *Astrophys. J. Suppl.* **155** (2004) 623–650 [[astro-ph/0403657](#)].
- [41] M. E. Gusakov, A. D. Kaminker, D. G. Yakovlev, and O. Y. Gnedin, *Enhanced cooling of neutron stars via Cooper-pairing neutrino emission*, *Astron. Astrophys.* **423** (2004) 1063–1072 [[astro-ph/0404002](#)].
- [42] D. Page, J. M. Lattimer, M. Prakash, and A. W. Steiner, *Neutrino Emission from Cooper Pairs and Minimal Cooling of Neutron Stars*, *Astrophys. J.* **707** (2009) 1131–1140 [[arXiv:0906.1621](#)].
- [43] O. Kargaltsev, G. G. Pavlov, and R. W. Romani, *Ultraviolet emission from the millisecond pulsar j0437-4715*, *Astrophys. J.* **602** (2004) 327–335 [[astro-ph/0310854](#)].
- [44] R. P. Mignani, G. G. Pavlov, and O. Kargaltsev, *A possible optical counterpart to the old nearby pulsar J0108-1431*, *Astron. Astrophys.* **488** (2008) 1027 [[arXiv:0805.2586](#)].
- [45] M. Durant, *et al.*, *The spectrum of the recycled PSR J0437-4715 and its white dwarf companion*, *Astrophys. J.* **746** (2012) 6 [[arXiv:1111.2346](#)].
- [46] B. Rangelov, *et al.*, *Hubble Space Telescope Detection of the Millisecond Pulsar J2124-3358 and its Far-ultraviolet Bow Shock Nebula*, *Astrophys. J.* **835** (2017) 264 [[arXiv:1701.00002](#)].
- [47] G. G. Pavlov, *et al.*, *Old but still warm: Far-UV detection of PSR B0950+08*, *Astrophys. J.* **850** (2017) 79 [[arXiv:1710.06448](#)].
- [48] V. Abramkin, Y. Shibano, R. P. Mignani, and G. G. Pavlov, *Hubble Space Telescope Observations of the Old Pulsar PSR J0108-1431*, *Astrophys. J.* **911** (2021) 1 [[arXiv:2103.00332](#)].
- [49] V. Abramkin, G. G. Pavlov, Y. Shibano, and O. Kargaltsev, *Thermal and Nonthermal Emission in the Optical-UV Spectrum of PSR B0950+08**, *Astrophys. J.* **924** (2022) 128 [[arXiv:2111.08801](#)].
- [50] D. Gonzalez and A. Reisenegger, *Internal Heating of Old Neutron Stars: Contrasting Different Mechanisms*, *Astron. Astrophys.* **522** (2010) A16 [[arXiv:1005.5699](#)].
- [51] K. Yanagi, N. Nagata, and K. Hamaguchi, *Cooling Theory Faced with Old Warm Neutron Stars: Role of Non-Equilibrium Processes with Proton and Neutron Gaps*, *Mon. Not. Roy. Astron. Soc.* **492** (2020) 5508–5523 [[arXiv:1904.04667](#)].

- [52] M. Fujiwara, K. Hamaguchi, N. Nagata, and M. E. Ramirez-Quezada, *Vortex creep heating in neutron stars*, *JCAP* **03** (2024) 051 [[arXiv:2308.16066](#)].
- [53] C. O. Heinke and W. C. G. Ho, *Direct Observation of the Cooling of the Cassiopeia A Neutron Star*, *Astrophys. J. Lett.* **719** (2010) L167–L171 [[arXiv:1007.4719](#)].
- [54] B. Posselt, G. G. Pavlov, V. Suleimanov, and O. Kargaltsev, *New constraints on the cooling of the Central Compact Object in Cas A*, *Astrophys. J.* **779** (2013) 186 [[arXiv:1311.0888](#)].
- [55] B. Posselt and G. G. Pavlov, *The Cooling of the Central Compact Object in Cas A from 2006 to 2020*, *Astrophys. J.* **932** (2022) 83 [[arXiv:2205.06552](#)].
- [56] P. S. Shternin, D. D. Ofengeim, C. O. Heinke, and W. C. G. Ho, *Constraints on neutron star superfluidity from the cooling neutron star in Cassiopeia A using all Chandra ACIS-S observations*, *Mon. Not. Roy. Astron. Soc.* **518** (2022) 2775–2793 [[arXiv:2211.02526](#)].
- [57] C. Heinke, *A Brief, Biased View of Neutron Star Cooling*, *Astron. Nachr.* **346** (2025) e20240110.
- [58] D. Page, M. Prakash, J. M. Lattimer, and A. W. Steiner, *Rapid Cooling of the Neutron Star in Cassiopeia A Triggered by Neutron Superfluidity in Dense Matter*, *Phys. Rev. Lett.* **106** (2011) 081101 [[arXiv:1011.6142](#)].
- [59] P. S. Shternin, D. G. Yakovlev, C. O. Heinke, W. C. G. Ho, and D. J. Patnaude, *Cooling neutron star in the Cassiopeia~A supernova remnant: Evidence for superfluidity in the core*, *Mon. Not. Roy. Astron. Soc.* **412** (2011) L108–L112 [[arXiv:1012.0045](#)].
- [60] M. J. P. Wijngaarden, *et al.*, *Diffusive nuclear burning in cooling simulations and application to new temperature data of the Cassiopeia A neutron star*, *Mon. Not. Roy. Astron. Soc.* **484** (2019) 974–988 [[arXiv:1901.01012](#)].
- [61] P. S. Shternin, *et al.*, *Model-independent constraints on superfluidity from the cooling neutron star in Cassiopeia A*, *Mon. Not. Roy. Astron. Soc.* **506** (2021) 709–726 [[arXiv:2106.05692](#)].
- [62] W. C. G. Ho, *et al.*, *X-ray bounds on cooling, composition, and magnetic field of the Cassiopeia A neutron star and young central compact objects*, *Mon. Not. Roy. Astron. Soc.* **506** (2021) 5015–5029 [[arXiv:2107.08060](#)].
- [63] E. Flowers, M. Ruderman, and P. Sutherland, *Neutrino pair emission from finite-temperature neutron superfluid and the cooling of young neutron stars*, *Astrophys. J.* **205** (1976) 541.
- [64] D. N. Voskresensky and A. V. Senatorov, *Emission of Neutrinos by Neutron Stars*, *Sov. Phys. JETP* **63** (1986) 885–897.

- [65] D. N. Voskresensky and A. V. Senatorov, *Description of Nuclear Interaction in Keldysh's Diagram Technique and Neutrino Luminosity of Neutron Stars. (In Russian)*, Sov. J. Nucl. Phys. **45** (1987) 411.
- [66] S.-H. Yang, C.-M. Pi, and X.-P. Zheng, *Rapid cooling of neutron star in Cassiopeia A and r -mode damping in the core*, *Astrophys. J. Lett.* **735** (2011) L29 [[arXiv:1103.1092](#)].
- [67] R. Negreiros, S. Schramm, and F. Weber, *Impact of Rotation-Driven Particle Repopulation on the Thermal Evolution of Pulsars*, *Phys. Lett. B* **718** (2013) 1176–1180 [[arXiv:1103.3870](#)].
- [68] D. Blaschke, H. Grigorian, D. N. Voskresensky, and F. Weber, *On the Cooling of the Neutron Star in Cassiopeia A*, *Phys. Rev. C* **85** (2012) 022802 [[arXiv:1108.4125](#)].
- [69] T. Noda, *et al.*, *Cooling of Compact Stars with Color Superconducting Phase in Quark Hadron Mixed Phase*, *Astrophys. J.* **765** (2013) 1 [[arXiv:1109.1080](#)].
- [70] A. Sedrakian, *Rapid cooling of the compact star in Cassiopeia A as a phase transition in dense QCD*, *Astron. Astrophys.* **555** (2013) L10 [[arXiv:1303.5380](#)].
- [71] D. Blaschke, H. Grigorian, and D. N. Voskresensky, *Nuclear medium cooling scenario in the light of new Cas A cooling data and the $2M_{\odot}$ pulsar mass measurements*, *Phys. Rev. C* **88** (2013) 065805 [[arXiv:1308.4093](#)].
- [72] A. Bonanno, M. Baldo, G. F. Burgio, and V. Urpin, *The neutron star in Cassiopeia A: equation of state, superfluidity, and Joule heating*, *Astron. Astrophys.* **561** (2014) L5 [[arXiv:1311.2153](#)].
- [73] L. B. Leinson, *Superfluid phases of triplet pairing and rapid cooling of the neutron star in Cassiopeia A*, *Phys. Lett. B* **741** (2015) 87–91 [[arXiv:1411.6833](#)].
- [74] G. Taranto, G. F. Burgio, and H. J. Schulze, *Cassiopeia A and direct URCA cooling*, *Mon. Not. Roy. Astron. Soc.* **456** (2016) 1451–1458 [[arXiv:1511.04243](#)].
- [75] H. Grigorian, D. N. Voskresensky, and D. Blaschke, *Influence of the stiffness of the equation of state and in-medium effects on the cooling of compact stars*, *Eur. Phys. J. A* **52** (2016) 67 [[arXiv:1603.02634](#)].
- [76] S. Tsiopelas and V. Sagun, *Neutron star cooling within the equation of state with induced surface tension*, *Particles* **3** (2020) 693–705 [[arXiv:2006.06351](#)].
- [77] D. K. Hong, C. S. Shin, and S. Yun, *Cooling of young neutron stars and dark gauge bosons*, *Phys. Rev. D* **103** (2021) 123031 [[arXiv:2012.05427](#)].
- [78] L. B. Leinson, *Hybrid cooling of the Cassiopeia A neutron star*, *Mon. Not. Roy. Astron. Soc.* **511** (2022) 5843–5848 [[arXiv:2202.08971](#)].
- [79] A. Ávila, E. Giangrandi, V. Sagun, O. Ivanytskyi, and C. Providência, *Rapid neutron star cooling triggered by dark matter*, *Mon. Not. Roy. Astron. Soc.* **528** (2024) 6319–6328 [[arXiv:2309.03894](#)].

- [80] H.-F. Zhu, G.-Z. Liu, and X. Wu, *Rapid cooling of the Cassiopeia A neutron star due to superfluid quantum criticality*, [arXiv:2410.21945](#) (2024).
- [81] J. Keller and A. Sedrakian, *Axions from cooling compact stars*, *Nucl. Phys. A* **897** (2013) 62–69 [[arXiv:1205.6940](#)].
- [82] N. N. Bogolyubov, *On a New method in the theory of superconductivity*, *Nuovo Cim.* **7** (1958) 794–805.
- [83] J. G. Valatin, *Comments on the theory of superconductivity*, *Nuovo Cim.* **7** (1958) 843–857.
- [84] E. M. Lifshitz and L. P. Pitaevskii, *Statistical Physics, Part 2*, vol. 9 of *Course of Theoretical Physics*. Butterworth-Heinemann, Oxford, 1980.
- [85] G. Grilli di Cortona, E. Hardy, J. Pardo Vega, and G. Villadoro, *The QCD axion, precisely*, *JHEP* **01** (2016) 034 [[arXiv:1511.02867](#)].
- [86] A. D. Kaminker, P. Haensel, and D. G. Yakovlev, *Neutrino emission due to proton pairing in neutron stars*, *Astron. Astrophys.* **345** (1999) L14–L16 [[astro-ph/9904166](#)].
- [87] <http://www.astroscu.unam.mx/neutrones/NSCool/>.
- [88] E. E. Kolomeitsev and D. N. Voskresensky, *Neutrino emission due to Cooper-pair recombination in neutron stars revisited*, *Phys. Rev. C* **77** (2008) 065808 [[arXiv:0802.1404](#)].
- [89] A. Akmal, V. R. Pandharipande, and D. G. Ravenhall, *The Equation of state of nucleon matter and neutron star structure*, *Phys. Rev. C* **58** (1998) 1804–1828 [[nucl-th/9804027](#)].
- [90] S. Goriely, N. Chamel, and J. M. Pearson, *Further explorations of Skyrme-Hartree-Fock-Bogoliubov mass formulas. XII: Stiffness and stability of neutron-star matter*, *Phys. Rev. C* **82** (2010) 035804 [[arXiv:1009.3840](#)].
- [91] J. M. Pearson, *et al.*, *Unified equations of state for cold non-accreting neutron stars with Brussels–Montreal functionals – I. Role of symmetry energy*, *Mon. Not. Roy. Astron. Soc.* **481** (2018) 2994–3026 [[arXiv:1903.04981](#)]. [Erratum: *Mon. Not. Roy. Astron. Soc.* 486, 768 (2019)].
- [92] J. M. Pearson, S. Goriely, and N. Chamel, *Properties of the outer crust of neutron stars from Hartree-Fock-Bogoliubov mass models*, *Phys. Rev. C* **83** (2011) 065810.
- [93] <http://www.ioffe.ru/astro/NSG/BSk/index.html>.
- [94] M. C. Miller *et al.*, *The Radius of PSR J0740+6620 from NICER and XMM-Newton Data*, *Astrophys. J. Lett.* **918** (2021) L28 [[arXiv:2105.06979](#)].
- [95] J. M. C. Chen, J. W. Clark, R. D. Davé, and V. V. Khodel, *Pairing gaps in nucleonic superfluids*, *Nucl. Phys. A* **555** (1993) 59–89.